Distributed RF Tomography for Tunnel Detection: Suitable Inversion Schemes

Lorenzo Lo Monte
General Dynamics
5100 Springfield Pike Ste. 504,
Dayton, OH 45431
Lorenzo.Lomonte@gdit.com

Danilo Erricolo,
Vittorio Picco
University of Illinois at Chicago
851 S. Morgan Ave,
Chicago, IL 60607
Erricolo@ece.uic.edu

Francesco Soldovieri
Consiglio Nazionale Ricerche
Via Diocleziano 328
Naples, Italy 80124
Soldovieri.f@irea.cnr.it

Michael C. Wicks
Air Force Research Laboratory
26 Electronics Parkway,
Rome, NY 13441
Michael.Wicks@rl.af.mil

***Abstract*— Distributed Radio Frequency (RF) Tomography is a novel approach for detecting underground tunnels and caves, over relatively wide areas. This method requires a set of affordable transmitters and receivers randomly deployed above the ground. Using the principles of inverse scattering, it is possible to develop a simplified theory for imaging below ground, thus revealing and locating voids. In this paper, we introduce inversion schemes suited for ground penetrating radar tomography applied to sensors that are randomly distributed over the area of interest.**

I. INTRODUCTION

In this work, we address the incumbent problem of detection, localization and monitoring of man-made tunnels, caves, bunkers, weapon caches, underground facilities (UGF) over relatively wide and deep regions of interest, for both cooperative and non-cooperative (denied) terrains. In military applications, the pursuit of "situational awareness" for the decision maker is paramount for successful dominance of the scene, especially for reconnaissance / discovery of UGF shafts or adits. Similarly, homeland defense and governing bodies need different but equally ubiquitous information to make effective decisions regarding disaster response and relief activities. Additionally, the engineering and scientific community may benefit from the increased information concerning the underground scene, e.g. for protection of national borders, surveillance of sensitive areas (such as prisons, banks, and nuclear power plants), mining industry and safety, geotechnology, environmental engineering, geophysics, archaeology and speleology. According to the *Layered Sensing* philosophy [1], the delivery of timely, actionable, trusted, persistent and relevant information of the below-ground scene, provided with affordable architectures and minimal resource allocation and human intervention, is imperative for the accomplishment of situational awareness. Although imaging below-ground targets is presently supplied by a plethora of methods, ranging from seismic to electromagnetic waves, or from gravity to optics, from impedance tomography to magnetotellurics, no technique complies with the guidelines prescribed by Layered Sensing. Amid those techniques, Ground Penetrating Radar deserves particular attention. Recent integration of diffraction tomography with classical GPR [2]-[8] augmented the potential target resolution. However, several aspects are challenging the compatibility of GPR with Layered Sensing:

- Classical GPR resolution is generally improved by using large bandwidth, oftentimes requiring high frequencies. However, due to soil properties, higher frequencies experience higher attenuations, and the increased frequency/bandwidth affects the signal to noise ratio (SNR) and intensifies dispersion effects.
- Systems using lower frequencies require electrically small wideband radiators, which results in complex wideband systems; yet, they may not provide adequate resolution to determine the geometry of targets.
- The allocable frequency spectrum is severely limited by interference with unintentional (e.g. broadcasting stations) or intentional (e.g. jammers) external radio sources; therefore, a reliable system must operate using a small, discrete and selectable number of frequencies.
- Any GPR survey requires the operator to be above the area under investigation.

This work was supported in part by Air Force Research Laboratory under contract #F33601-02-F-A58, and by the Department of Defense under grant #FA9550-05-1-0443.

978-1-4244-4495-3/09/$25.00 ©2009 IEEE

Report Documentation Page

Form Approved
OMB No. 0704-0188

1. REPORT DATE	2. REPORT TYPE	3. DATES COVERED
JUL 2009		**00-00-2009 to 00-00-2009**

4. TITLE AND SUBTITLE	5a. CONTRACT NUMBER
Distributed RF Tomography for Tunnel Detection: Suitable Inversion Schemes	5b. GRANT NUMBER
	5c. PROGRAM ELEMENT NUMBER
6. AUTHOR(S)	5d. PROJECT NUMBER
	5e. TASK NUMBER
	5f. WORK UNIT NUMBER
7. PERFORMING ORGANIZATION NAME(S) AND ADDRESS(ES) **Air Force Research Laboratory,26 Electronics Parkway,Rome,NY,13441**	8. PERFORMING ORGANIZATION REPORT NUMBER
9. SPONSORING/MONITORING AGENCY NAME(S) AND ADDRESS(ES)	10. SPONSOR/MONITOR'S ACRONYM(S)
	11. SPONSOR/MONITOR'S REPORT NUMBER(S)

12. DISTRIBUTION/AVAILABILITY STATEMENT
Approved for public release; distribution unlimited

13. SUPPLEMENTARY NOTES
IEEE National Aerospace and Electronics Conference (NAECON), Fairborn, OH, Jul. 2009.

14. ABSTRACT
Distributed Radio Frequency (RF) Tomography is a novel approach for detecting underground tunnels and caves over relatively wide areas. This method requires a set of affordable transmitters and receivers randomly deployed above the ground. Using the principles of inverse scattering, it is possible to develop a simplified theory for imaging below ground, thus revealing and locating voids. In this paper, we introduce inversion schemes suited for ground penetrating radar tomography applied to sensors that are randomly distributed over the area of interest. 1

15. SUBJECT TERMS

16. SECURITY CLASSIFICATION OF:			17. LIMITATION OF ABSTRACT	18. NUMBER OF PAGES	19a. NAME OF RESPONSIBLE PERSON
a. REPORT **unclassified**	b. ABSTRACT **unclassified**	c. THIS PAGE **unclassified**	**Same as Report (SAR)**	**8**	

- Borehole GPR, which may increase the penetration depth, is generally expensive, subject to drilling misalignments and, most important, is impractical in inaccessible territories.
- Airborne GPR, which does not require substantial human intervention, is challenged by the strong reflection due to the air-earth interface, which completely masks the weak scattered signal from buried voids.

To date, no underground imaging system conforms to Layered Sensing. Hence, the development of an innovative architecture is mandatory.

II. RF TOMOGRAPHY

To address these unresolved problems, a new wide area / deep range below-ground imaging of high contrast dielectric / conducting anomalies, based upon a *distributed* architecture, is introduced [9]-[10]. In this context, the *view* (associated with the different transmitters) and the *observation* (associated with different receivers) diversity increases the information pertaining to the scene, while reducing the necessity of a large spectral content of the probing waveform: in principle, using just a single frequency, range-independent and subwavelength resolution images are feasible.

This distributed scheme, based on the principles of *RF Tomography*, considers two separate sets of *N* electromagnetic transmitters (Tx) and *M* electromagnetic receivers (Rx), commonly referred with the generic name of *Transponder*. These transponders are placed on (or in) the ground at an *arbitrary* and *discretionary* position, including random deployment. The transmitter Tx radiates a known waveform using a suitable polarization. The probing wave impinges upon a buried dielectric / conductive anomaly, thus generating a scattered wave-field. The distributed receivers collect samples of the scattered instantaneous electric field, and estimate the complex-valued electric field phasor at their locations. Subsequently, this information is relayed to the overlying base station. To ease the detection process, one transmitter and frequency of operation are activated per time, thus simplifying the receiver's capability to properly discern the origin of the incoming wave-field. For a given sampling time, the used spectrum is virtually restricted to a single frequency component, thus ensuring ultra-narrowband system architecture, low noise and affordable cost. To expedite the set-up and portability of the system, sensors are intended to be "dart" shaped. Sensors may be equipped with built-in GPS for precision timing and positioning, and a S-Band communication link to transfer the collected data to a overhead base station. During the sensor dissemination phase, transponders may fall in obstructed regions, or in region where clutter is excessive (e.g. Tx and Rx lay in proximity, or over a vegetation layer) and presumably they may default. In any case, the proposed image reconstruction process accounts for the eventual failure or obstruction of transponders, by properly neglecting corrupted sensors.

RF Tomography may also operate using a discrete set of monochromatic frequency components, selected according to environmental conditions. A suitable modulation scheme is the stepped FM; however, in this report the conclusions are independent from the type of modulation implemented. The choice of the operating frequencies must facilitate the penetration of electromagnetic waves into the ground, while simultaneously maintaining acceptable detection and resolution capabilities. Higher frequencies yield better resolution, but strong attenuation limits the range of operation. Conversely, the corresponding resolution obtainable using lower frequencies may not be adequate to localize tunnels, and the field behavior becomes diffusive, thus reducing the back-scattered field. A suitable range of frequencies for this application is found to be the range 1-15MHz. Nevertheless, the final frequency selection strictly depends on the expected target type and/or depth. Note that in HF range the radiators can be approximated as electrically small dipoles or loops, enabling the possibility to incorporate the radiator's antenna pattern directly in the signal processing model. RF Tomography offers numerous advantages that technically outperform any currently available system for below-ground imaging. Indeed, RF tomography complies in full with the requirements established by Layered Sensing. Some reasons are explained as follows.

Wide area / Deep Range: the use of HF frequencies, and that the tomographic theory still holds as long as the field does not behave as diffusive, implies that the probing wave-front penetrates the ground at very large depths. Furthermore, the burial of sensors, or their placement on top of the air-earth interface, drastically increases the amount of power injected into the ground. Assuming ideal conditions, 100 meters of depth and several thousands of square meters of area can be theoretically surveyed. Due to the natural spread of sensors over a wide area, the system is well suited for *horizontal prospecting*. The classical GPR diffraction tomography was unable to include depolarization effects that normally occur when the anomaly is considered high-contrast. Furthermore, diffraction tomography is not applicable when the host medium changes the polarization of the probing wave, as in the case of the air-earth interface. With the introduction of the *generalized diffraction tomography*, proposed in [7]-[15], the depolarization effect is accounted, thus yielding better reconstructed images. Moreover, the proposed forward model formulation considers the possibility of the sensors to be in the near field, thus allowing larger investigation areas, from very shallow to very deep regions. Therefore, the typical

problem of "blind" region that affects any radar-based system is virtually eliminated.

Actionable Deliverables: the forward model for RF tomography and the proposed generalized diffraction tomography have been developed by neglecting part of the information concerning the value of the dielectric permittivity and the shape of the targets, while preserving the information concerning the location and the overall extension of the object. Therefore, the proposed tomographic reconstruction procedure has been tailored to ease the process of *detection, identification, location, trace* and *reconnaissance* of underground bodies, thus providing the decision maker only with *intelligible, relevant* and *actionable* information.

Minimal Human Intervention: RF tomography is particularly suited for remote probing without the involvement of human resources. Considering a dangerous area, where humans would be in danger, one can still surround the area of interest with transponders (for example along a circle) and RF tomography can still provide relevant information of below ground entities. Furthermore, in the event that the area is completely inaccessible, sensors can be disseminated from an airborne vehicle, and below-ground images can be reconstructed in a very short amount of time.

Real Time: the time required by RF tomography to reconstruct an actionable image of below ground targets is the mere summation of the time needed for deploying sensors above the region of interest, and the time requested for data collection and retrieval. If sensors are dropped from an aircraft, and the data processing is performed via a high performance computer, then reconstructed images can be available in terms of minutes, and revisit time is measurable in terms of seconds.

Affordability: the design, manufacturing, testing and realization of transponders in the HF band are relatively simple and inexpensive procedures, and precise location, timing, and phase coherence can be guaranteed by the well established, standardized, and low-cost GPS technology.

Agility: differently from common geophysical survey methods, where regular grids are necessary to sample the data, RF tomography is developed in a way that the location of sensors is discretionary, and it may be completely random. Randomness of the sensor deployment does not preclude the system operability: at most, if sensors are poorly arranged in the ground, a slight degradation of the reconstructed image may be expected. By accounting for the possibility of default of transponders, the tomographic inversion procedure can be considered modular, and the sensing can be persistent. Furthermore, RF tomography is suited for detection of targets of any shape and from any sensor distribution. In fact, conventional radar systems are not able to detect targets whose backscattered RCS is equal to zero. In order to increase the detection probability, different waveforms, multistatic solutions or auto-focusing need to be implemented in the system. In RF Tomography, *any* particular value of the RCS is considered useful information, including the case when $RCS = 0$. Therefore, RF Tomography is virtually able to detect targets that, from some particular points of view, may have zero backscattered field, and use this information to accurately determine properties of the target.

Spectral Dominance: theoretically, RF tomography features the highest number of diversities among any other void detection system. In fact, RF tomography comprises frequency, polarization, waveform, code, modulation, antenna pattern, view, and observation diversities. RF tomography works in principle with a monochromatic waveform. Indeed, with the use of generalized diffraction tomography, the more the system is narrowband, the better the performance is. Since RF Tomography operates at a single frequency, it is not affected by frequency dispersion.

Resolution: The use of generalized diffraction tomography in our proposed system guarantees the sub-wavelength and range independent resolution. Current research concerning compressive sensing, time reversal and MUSIC algorithms may further improve the capability of discrimination among closely spaced targets, thus achieving the so-called super-resolution.

Robustness to Noise: in RF tomography the concept of "sample" is more elaborated than in classical radar theory, where samples are collected at different times, and then averaged, to increase the SNR. In our case, a "sample" may be defined as the particular combination of transmitter, receiver, frequency (or waveform), polarization, and time. Following this definition, for a given time, frequency of operation and polarization, we may expect a SNR increase proportional to the square root of the total number of Tx and Rx. By time averaging these results, the expected SNR can be arbitrarily increased according to the operator's demand. Although this unbounded improvement is not reached in real cases (because clutter cannot be modeled as Gaussian noise), it still gives an insight of the tremendous robustness to noise/clutter of RF tomography.

Persistent Sensing: the peculiar distributed sensing in RF tomography provides the user with profound situational awareness of the underground scene. Particularly, the persistence is guaranteed by the multitude of sensors, and the failure of some Tx/Rx units does not preclude the overall image reconstruction process.

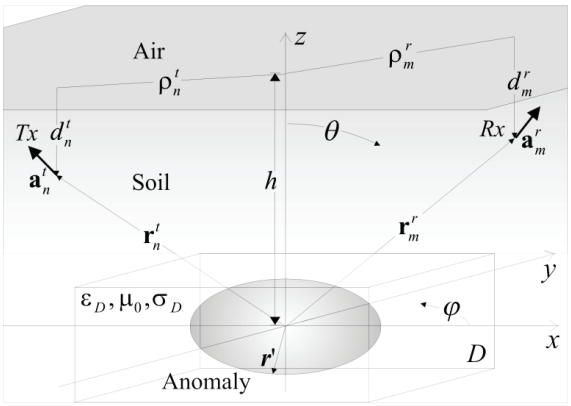

Figure 1. Geometric representation of RF Tomography

III. FORWARD MODEL

To derive a general framework for RF Tomography inversion algorithms, a suitable model for the electric field (closely representing the actual scattering process) needs to be defined. The 3D geometry of the problem is depicted in Fig. 1. For simplicity, a single operating frequency f is adopted, but extension to the multi-frequency operation is straightforward. Under the monochromatic assumption, the ground is modeled as a semi-space homogeneous medium with relative dielectric permittivity ε_D , conductivity σ_D, and magnetic permeability μ_0. The targets (i.e. tunnels or voids) are assumed to reside inside the investigation domain *D*, which is fully enclosed in the ground. The sources are *N* electrically small dipoles (of length Δl^t) or loops (of area A^t) fed with current I^t, and located at position $\mathbf{r}_n^t$ (view diversity), and having (electric or magnetic) dipole moment direction and polarization expressed by the complex valued unit-norm vector $\hat{\mathbf{a}}_n^t$. For each transmitting antenna, the scattered field $\mathbf{E}^S$ is collected by *M* receivers (observation diversity), located at $\mathbf{r}_m^r$ points in space, and having moment direction and polarization $\hat{\mathbf{a}}_m^r$. The unknowns of the problem are the relative dielectric permittivity profile $\varepsilon_r(\mathbf{r}')$ and the conductivity profile $\sigma(\mathbf{r}')$ inside the investigation domain *D*. The resulting inverse problem is cast in terms of the unknown permittivity contrast function:

$$\varepsilon_\delta(\mathbf{r}') = \varepsilon_r(\mathbf{r}') - \varepsilon_D - j\frac{\sigma(\mathbf{r}') - \sigma_D}{2\pi f \varepsilon_0}. \qquad (1)$$

The total instantaneous electric field experienced at the receiver in time domain has been derived in [10], [16]-[17]:

$$E(\mathbf{r}_n^t, \mathbf{r}_m^r, t) = \mathrm{Re}\left\{e^{-j\omega t}\left[Qk_0^2 \times \iiint_D \left[\mathbf{a}_m^r \cdot \underline{\underline{\mathbf{G}}}(\mathbf{r}_m^r, \mathbf{r}')\right] \cdot \left[\underline{\underline{\mathbf{G}}}(\mathbf{r}', \mathbf{r}_n^t) \cdot \mathbf{a}_n^t\right] \varepsilon_\delta(\mathbf{r}')\, d\mathbf{r}' + Q\mathbf{a}_m^r \cdot \underline{\underline{\mathbf{G}}}(\mathbf{r}_m^r, \mathbf{r}_n^t) \cdot \mathbf{a}_n^t + H(\mathbf{r}_m^r, \mathbf{r}_n^t)\right]\right\} + N(t) \qquad (2)$$

The term $\mathbf{a}_m^r \cdot \mathbf{G}(\mathbf{r}_m^r, \mathbf{r}_n^t) \cdot \mathbf{a}_n^t$ in eq. (2) represents the direct coupling between Tx and Rx, and it can be considered a source of deterministic clutter. The term $H(\mathbf{r}_m^r, \mathbf{r}_n^t)$ represents the non-linear contribution due to higher-order Born series terms. In the reconstruction process, $H(\mathbf{r}_m^r, \mathbf{r}_n^t)$ is considered as unknown static bias (clutter) to the desired signal. The random variable $N(t)$ represents the thermal noise and the quantization errors, and can be treated as a Gaussian process with zero mean.

RF Tomography presents the challenging problem of mitigation of the direct-path coupling between transponders. A simple strategy to mitigate the direct-path coupling consists in the constrained minimization of the electric field radiated from the transmitting antenna measured at the position of a particular receiver. Mathematically, the constrained minimization problem is recast in the following form: for each *n,m* pair,

$$\begin{aligned} &\text{minimize: } \left\| \underline{\underline{\mathbf{G}}}(\mathbf{r}_m^r, \mathbf{r}_n^t) \cdot \mathbf{a}_n^t \right\|_2^2 \\ &\text{subject to: } (\mathbf{a}_n^t)^T \cdot \mathbf{a}_n^t = 1 \end{aligned} \qquad (3)$$

This constrained minimization problem can be easily solved by constructing a series of Lagrangian forms:

$$\Lambda_{n,m}(\mathbf{a}_n^t, \lambda) = (\mathbf{a}_n^t)^T \cdot \underline{\underline{\mathbf{G}}}^*(\mathbf{r}_m^r, \mathbf{r}_n^t) \cdot \underline{\underline{\mathbf{G}}}(\mathbf{r}_m^r, \mathbf{r}_n^t) \cdot \mathbf{a}_n^t - \lambda\left[(\mathbf{a}_n^t)^T \cdot \mathbf{a}_n^t - 1\right] \qquad (4)$$

where $\mathbf{G}^*$ denotes the Hermitian of $\mathbf{G}$. By imposing $\nabla\Lambda = 0$ we obtain:

$$\underline{\underline{\mathbf{G}}}^*(\mathbf{r}_m^r, \mathbf{r}_n^t) \cdot \underline{\underline{\mathbf{G}}}(\mathbf{r}_m^r, \mathbf{r}_n^t) \cdot \mathbf{a}_n^t = \lambda \mathbf{a}_n^t \qquad (5)$$

Therefore, the $\mathbf{a}_n^t$ direction that minimized the power at a desired location is the eigenvector associated with the

smallest eigenvalue of the (positive semidefinite) matrix $\mathbf{G}^{*}\mathbf{G}$. Similarly, we can apply this minimization technique at the receiver side: by defining the vector quantity

$$\underline{E}_{\min} = \underline{\underline{\mathbf{G}}}\left(\mathbf{r}_m^r, \mathbf{r}_n^t\right) \cdot \mathbf{a}_n^t \tag{6}$$

as the electric field obtained when $\mathbf{a}_n^t$ is chosen according to (3), a second minimization problem can be formulated:

$$\begin{aligned} &\text{minimize} \quad \left\| \left(\mathbf{a}_m^r\right)^T \cdot \underline{E}_{\min} \right\|_2^2 \\ &\text{subject to:} \ \left(\mathbf{a}_m^r\right)^T \cdot \mathbf{a}_m^r \end{aligned} \tag{7}$$

The minimization is achieved when $\mathbf{a}_m^r$ is chosen to be the eigenvector corresponding to the smallest eigenvalue of the matrix $E_{\min} \cdot E_{\min}^{*}$.

As tested via numerical analysis, the application of these strategies guarantees an acceptable minimization of the received clutter, thus the total electric field (in phasor form) can be approximated with the scattered contribution from targets inside the region *D*,:

$$\begin{aligned} &E\left(\mathbf{r}_n^t, \mathbf{r}_m^r\right) \cong E^S\left(\mathbf{r}_n^t, \mathbf{r}_m^r\right) = \mathbf{L}\left(\varepsilon_\delta\left(\mathbf{r}'\right)\right) = Qk_0^2 \times \\ &\iiint_D \left[\mathbf{a}_m^r \cdot \underline{\underline{\mathbf{G}}}\left(\mathbf{r}_m^r, \mathbf{r}'\right)\right] \cdot \left[\underline{\underline{\mathbf{G}}}\left(\mathbf{r}', \mathbf{r}_n^t\right) \cdot \mathbf{a}_n^t\right] \varepsilon_\delta\left(\mathbf{r}'\right) d\mathbf{r}' \end{aligned} \tag{8}$$

IV. Inversion Strategies

The inversion algorithms are valid assuming that the direct path contribution and Gaussian noise are substantially mitigated, so that their contribution can be considered as perturbations on the measured data; therefore, the field received by the sensors is assumed to be the one described by the forward model in eq. (8). A way to compute the contrast function using (8) is to perform a numerical inversion of the integral operator. The sampled field can be collected in a vector $\underline{E} = \left\{E\left(\mathbf{r}_n^t, \mathbf{r}_m^r\right)\right\}$, of length NM, and the region *D* can be discretized in *K* voxels, each one located at position $\mathbf{r}_k'$: the contrast function can be embodied in a column vector $\underline{\varepsilon}_\delta = \left\{\varepsilon_\delta\left(\mathbf{r}_k'\right)\right\}$ of length *K*. After this discretization, eq. (8) can be rewritten in matrix form as:

$$\underline{E} = \underline{\underline{\mathbf{L}}}\,\underline{\varepsilon}_\delta, \tag{9}$$

Hence, the problem is to invert the relation (9). In eq. (9), $\mathbf{L}$ is a matrix with dimensions $NM \times K$, which is typically ill conditioned. The operator $\mathbf{L}$ is commonly reaching values of condition number κ greater than 10^6. This leads to artifacts in the reconstruction process, particularly exacerbated when noise (thermal, external, quantization), clutter or coupling is impinging upon the receivers.

According to the accuracy required from the system, several inversion strategies are proposed [10], [16]-[17]:

- *Levenberg-Marquardt* (LM) regularization procedure. This method is relatively accurate for any environmental condition and it is robust in presence of noise. It requires a proper choice of a regularization parameter.
- *Truncated Singular Value Decomposition* (TSVD). This method is also relatively accurate in any scenario and moderately resistant to noise interference. This method also offers deeper insight into the physics behind the reconstruction, and the output can be easily adjusted by properly selecting the number of meaningful singular values. The number of retained singular values in TSVD plays the same role of the LM regularization parameter.
- *Back Propagation* approach. This method works properly only when the operator $\mathbf{L}$ is well conditioned. This implies that it can be used only for particular configurations and when the SNR is relatively high. However, the computational time is drastically reduced.
- *Weighted LM and Weighted TSVD.* These strategies are natural extensions of LM and TSVD methods that include a proper weighting function of the sensors, in order to equalize the contribution due to a particular Tx and Rx pair. If speed is not a concern, weighted LM or weighted TSVD are the superlative choices.
- *Fourier-Bojarski* approach. This is the fastest inversion scheme and it is suited for far-field probing and quasi-lossless soils. It privileges speed instead of accuracy.
- *Sub-Space Models*, suited for increasing the resolution when very low frequencies are used and the targets can be approximated as being point-like.
- *Compressive Sensing*, suited when the number of transmitters and receivers (i.e. the number of samples) is limited.

The mathematical description of the first four methods is presented in [10], [16-17]. In this work, we will discuss more in detail the last 3 approaches.

A. *Weighted Regulatization Methods*

Weighted methods are based upon the assumption that the insertion of weighing matrices opportunely defined may equalize the information content provided by each Tx-Rx pair. For instance, the weighted version of the LM method can be reformulated as follows [16-17]:

$$\hat{\underline{\underline{\varepsilon}}}_{\delta}\left(\beta\right)=\left(\mathbf{L}^{*}\mathbf{W}_{E}^{2}\mathbf{L}+\beta\mathbf{W}_{\varepsilon}^{2}\right)^{-1}\left(\mathbf{L}^{*}\mathbf{W}_{E}^{2}\underline{\underline{E}}+\beta\mathbf{W}_{\varepsilon}^{2}\underline{\underline{\varepsilon}}_{\delta}^{0}\right) \quad (10)$$

where $\underline{\underline{\varepsilon}}_{\delta}^{0}$ represents the known dielectric anomalies embedded in region D, and

$$\mathbf{W}_{\varepsilon}=\mathrm{diag}\left(\mathbf{L}^{*}\mathbf{L}\right)^{1/2} \quad (11)$$

$$\mathbf{W}_{E}=\mathrm{diag}\left(\mathbf{L}\mathbf{L}^{*}\right)^{1/2} \quad (12)$$

are (diagonal) the weighting matrices, opportunely defined in order to minimize the *sensitivity* of the system [2].

In most cases, the weighting matrices have a small dynamic range. Therefore, we can approximate $\mathbf{W}_{\varepsilon}\cong\alpha\mathbf{I}$ in the matrix inversion term of eq. (10). If we perform the singular value decomposition [11] of a weighed matrix $\mathbf{L}_{w}$ defined as:

$$\underline{\underline{\mathbf{L}}}_{w}=\mathbf{W}_{E}\mathbf{L}=\underline{\underline{\mathbf{U}}}\,\underline{\underline{\mathbf{S}}}\,\underline{\underline{\mathbf{V}}}^{*} \quad (13)$$

we can rewrite (10) in terms of (13), obtaining:

$$\begin{aligned}\hat{\underline{\underline{\varepsilon}}}_{\delta}&=\left(\mathbf{L}_{w}^{*}\mathbf{L}_{w}+\beta\mathbf{W}_{\varepsilon}^{2}\right)^{-1}\left(\mathbf{L}_{w}^{*}\mathbf{W}_{E}\underline{\underline{E}}+\beta\mathbf{W}_{\varepsilon}^{2}\underline{\underline{\varepsilon}}_{\delta}^{0}\right)\\&\cong\left(\mathbf{V}\mathbf{S}^{*}\mathbf{S}\mathbf{V}^{*}+\alpha^{2}\beta\mathbf{I}\right)^{-1}\left(\mathbf{V}\mathbf{S}^{*}\mathbf{U}^{*}\mathbf{W}_{E}\underline{\underline{E}}+\beta\mathbf{W}_{\varepsilon}^{2}\underline{\underline{\varepsilon}}_{\delta}^{0}\right) \quad (14)\\&=\mathbf{V}\mathrm{diag}\left(\frac{1}{s_{i}^{2}+\alpha^{2}\beta}\right)\left(\mathbf{S}^{*}\mathbf{U}^{*}\mathbf{W}_{E}\underline{\underline{E}}+\mathbf{V}^{*}\beta\mathbf{W}_{\varepsilon}^{2}\underline{\underline{\varepsilon}}_{\delta}^{0}\right)\end{aligned}$$

where s_{i} represent the i-th singular value of $\mathbf{L}_{w}$. The advantage obtained in applying eq. (14) is that the contrast function as function of β can be computed via (fast) matrix multiplications.

B. *Time Reversal and Sub-Space Method*

Sub-space methods, such as the *MUSIC* algorithm, are appealing when the probing frequency is very low, where improving resolution is the main challenge. The lower the frequency, the more the tunnels resemble point scatterers, therefore imaging via the *MUSIC* algorithm may be possible. The first step is to use all transmitters simultaneously. We fill the multistatic response matrix in the following manner:

$$K\left(\mathbf{r}'_{k}\right)=k_{0}^{2}Q\begin{bmatrix}G_{Tx1}G_{Rx1} & \cdots & G_{Tx1}G_{RxM}\\ \vdots & \ddots & \vdots\\ G_{TxN}G_{Rx1} & \cdots & G_{TxN}G_{RxM}\end{bmatrix}, \quad (15)$$

where

$$\begin{aligned}G_{Txn}&=G\left(\mathbf{r}'_{k},\mathbf{r}_{n}^{t}\right)\\G_{Rxm}&=G\left(\mathbf{r}_{m}^{r},\mathbf{r}'_{k}\right)\end{aligned}. \quad (16)$$

We define "Green's function vector" (or steering vector) the vector entries in (15):

$$g\left(\mathbf{r}'_{k}\right)=\begin{bmatrix}G_{Tx1}G_{Rx1} & \cdots & G_{TxN}G_{Rx1}\end{bmatrix}^{T} \quad (17)$$

It has been shown [18] that the eigenvectors of the matrix

$$T=K^{H}K \quad (18)$$

corresponds in a one-to-one manner to different targets (when targets are well-resolved). In particular, the wavefront generated by the array, when excited by one of these eigenvectors, focuses on the associated target so that a synthetic image of the target locations is easily computed. This procedure is commonly referred to as "*Time Reversal*" [18]. However, it is known that time reversal shows poor performance when the array is sparse (which is, unfortunately, our case). A way to improve the reconstruction quality and lead to super resolved images is to apply the *MUSIC* algorithm to the matrix *T*. The *MUSIC* algorithm makes use of the fact that the time-reversal matrix *T* is a projection operator onto the subspace spanned by the complex conjugates of the Green function vectors of *K* (the signal sub-space) and that the noise subspace is spanned by the eigenvectors of *T* having zero eigenvalue. It then follows that the complex conjugate of each Green function vector must be orthogonal to the noise subspace and, in particular, to the eigenvectors of the *T* matrix [18]. We define the *MUSIC* pseudo-spectrum as:

$$D\left(\hat{\mathbf{r}}'_{k}\right)=\frac{1}{\sum_{p}\left|\left\langle\underline{\tau}_{p},g\left(\mathbf{r}'_{k}\right)\right\rangle\right|^{2}} \quad (19)$$

where $\underline{\tau}_{p}$ are the eigenvectors of *T* having zero eigenvalue. According to *MUSIC* algorithm, peaks of *D* reveal the actual target locations.

C. Compressive Sensing

Compressive sensing (CS) is a concept formally introduced by Candes et al. [19], and Donoho [20] to overcome the Shannon/Nyquist restriction on the sampling period. Recently, the scientific community has discovered its potentialities to many applications, including imaging. In fact, problems in compressive sensing are generally formulated as constrained minimization of matrix equations.
Using our notation, a typical compressive sensing problem is recast in terms of the following minimization:

$$\begin{aligned} &\text{minimize} \quad \left\| \underline{\underline{\varepsilon}}_{\delta} \right\|_p \\ &\text{subject to} \quad \underline{\underline{\mathbf{L}}}\,\underline{\underline{\varepsilon}}_{\delta} = \underline{\underline{E}}_S \end{aligned} \tag{20}$$

where the norm used for the minimization is represented by *p*. With respect to others "standard" implementation of CS, we are not building a sampling matrix, but we are using the matrix **L** as it is obtained from the forward model. When *p=2* the minimization problem is identical to the classical Tikhonov regularization procedure. However, when *p=1* or *p=0* the solution of the constrained minimization shows the peculiar feature of having a greater number of zero-valued pixels. This leads to high-contrast, sharper and low-blurred images with respect to classical regularization procedures. This result can be used also in a different way: using compressive sensing, the same image quality is expected using fewer samples, which in turns may save the system complexity and cost. Three algorithms typical of compressive sensing are investigated: Basis Pursuit [21]-[22], Orthogonal Matching Pursuit [23], and Homotopy/LASSO [24]-[25].

V. SIMULATIONS

Simulations are performed using two different environments:

1) Random distribution. The simulation intends to mimic the case in which sensors are randomly deployed above an area of interest. Targets are expected to be located below the transponders.

2) Close-In Sensing. The simulation intends to replicate the case in which a denied area needs to be explored. Therefore, sensors are surrounding the area of interest, and images are reconstructed by exploitation of lateral waves.
Preliminary results are shown in Figs. 4-5, where the two tunnels can be easily recognized. Details regarding the simulation are found in [10]. Further results and comparisons will be shown at the time of the conference.

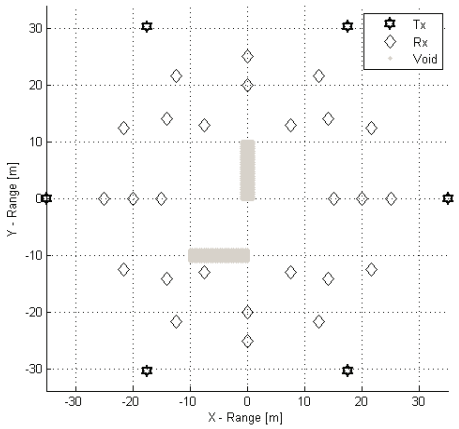

Figure 2. Sensor disposition for the case 1.

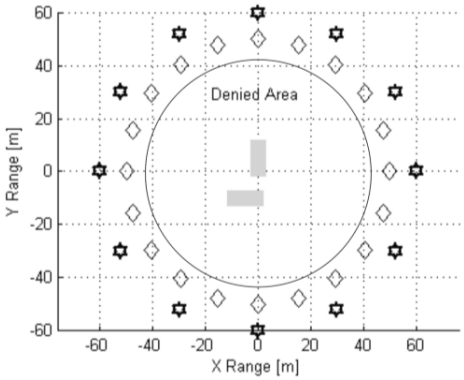

Figure 3. Sensor disposition for the case 2

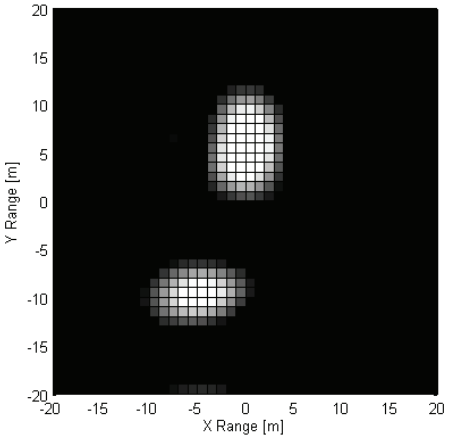

Figure 4: Reconstructed image using TSVD and scattered field data generated using the forward model in Section II and the geometry depicted in Fig.2

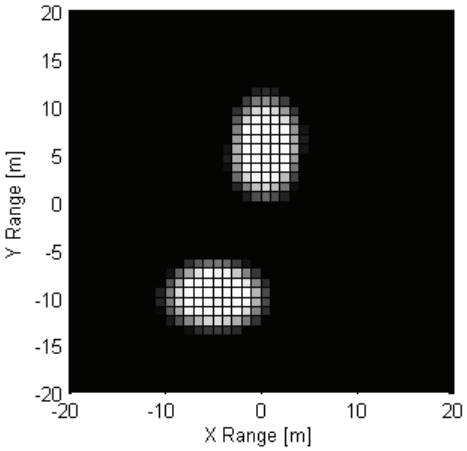

Figure 5: Reconstructed image using TSVD and scattered field data generated using the forward model in Section II and the geometry depicted in Fig.3

VI. ACKNOWLEDGEMENTS

The authors are thankful to Mr. W. J. Baldygo, Air Force Research Laboratory, and Dr. J. A. Sjogren, Air force Office of Scientific Research, for sponsoring and funding this research.

REFERENCES

[1] M. Bryant, P. Johnson, B. M. Kent, M. Nowak, S. Rogers, "Layered Sensing: its definition, attributes, and guiding principles for AFRL strategic technology development," online document, URL: www.wpafb.af.mil/shared/media/document/AFD-080820-005.pdf

[2] R.J. Lytle, E.F Laine, D.L. Lager and D.J. Davis "Using Cross Borehole Electromagnetic Probing to Locate High Contrast Anomalies," Geophysics. Vol. 44, pp. 1667-1676, 1979.

[3] A.J Devaney, "Geophysical Diffraction Tomography" IEEE Trans on Geosci. Remote Sens. Vol. GE-22, No. 1, pp. 3-13, Jan. 1984.

[4] A.J. Witten, J.E. Molyneux, J.E. Nyquist, "Ground Penetrating Radar Tomography: Algorithms and Case Studies," *IEEE Trans. Geosci. Remote Sens.*, Vol 32, No. 2, pp. 461-467, Mar. 1994.

[5] A.J. Witten, and E. Long, "Shallow Applications of Geophysical Diffraction Tomography". *IEEE Transactions on Geoscience and Remote Sens.*, Vol. 24, No. 5, p. 654-662, Sept. 1986

[6] T. B. Hansen, and P. M. Johansen, "Inversion Scheme for Ground Penetrating Radar that Takes Into Account the Planar Air-Soil Interface," *IEEE Trans. Geosci. Remote Sens.*, Vol. 38, No. 1, pp. 496-506, Jan. 2000

[7] T. J. Cui and W. C. Chew, "Diffraction Tomographic Algorithm for the Detection of Three-Dimensional Objects Buried in a Lossy Half-Space," *IEEE Transactions on Antennas and Propagation.* Vol. 50, No. 1, pp. 42-49, Jan. 2002.

[8] P. Meincke, "Linear GPR Inversion for Lossy Soil and a Planar Air-Soil Interface," *IEEE Trans. Geosci. and Remote Sens.*, Vol 39, No. 12, pp. 2713-2721, Dec. 2001

[9] M. C. Wicks, "RF Tomography with Application to Ground Penetrating Radars," IEEE *Proc. 41st Asilomar Conference ACSSC 2007*, pp. 2017-2022, 4-7 Nov. 2007.

[10] L. Lo Monte, D. Erricolo, F. Soldovieri, M. C. Wicks, "Radio Frequency Tomography for Tunnel Detection," *IEEE Trans. Geosci. Remote Sens.*, in press.

[11] G. Leone, F. Soldovieri, "*Analysis of the distorted Born approximation for Subsurface Reconstruction: Truncation and Uncertainities Effect,"* IEEE Trans. on Geosci. and Remote Sens., Vol. 41, No. 1, pp. 66-74, Jan. 2003

[12] R. Persico, R. Bernini, F. Soldovieri, "The Role of the Measurement Configuration in Inverse Scattering from Buried Objects under the Born Approximation," *IEEE Trans on Antennas Propag.*, Vol. 53, No. 6, pp. 1875-1887, Jun 2005

[13] H. J. Li and F. L. Lin, "A Generalized Interpretation and Prediction in Microwave Imaging Involving Frequency and Angular Diversity," *J. Electromagnetic Waves and Applications*, Vol. 4, No. 5, pp. 415-430, 1990

[14] F. Soldovieri, J. Hugenschmidt, R. Persico, G. Leone, "A Linear Inverse Scattering Algorithm for Realistic GPR Applications," *Near Surface Geophysics*, Vol. 5, No. 1, pp. 29-42, Feb. 2007

[15] W.C. Chew, *Waves and Fields in Inhomogeneous Media*. IEEE Press, 1995, Piscataway NJ

[16] M. S. Zhdanov, *Geophysical Inverse Theory and Regularization Problems*, Methods in Geochemistry and Geophysics, Vol. 36, Elsevier, Amsterdam, 2002.

[17] M. S. Zhdanov, *Geophysical Electromagnetic Theory and Methods*, Vol. 43, Elsevier Science, Amsterdam, the Netherland, 2009.

[18] A.J. Devaney, "Time Reversal Imaging of Obscured Targets from Multistatic Data," *IEEE Trans. Antennas Propag.*, Vol 53, No. 5, May 2005

[19] R. T. Candes, "Robust uncertainty principles: exact signal reconstruction from highly incomplete frequency information," *IEEE Trans. Info. Theory*, Vol. 52, No. 2, 2006.

[20] D. Donoho, "Compressed Sensing," *IEEE Trans. Info. Theory*, Vol. 52, No. 4, 2006.

[21] S. S. Chen, D. L. Donoho, M. A. Saunders, "Atomic Decomposition by Basis Pursuit," *Society for Industrial and Applied Mathematics*, 2001.

[22] S. S. Chen, D. L. Donoho, "Basis pursuit", *Conference Record of the Twenty-Eighth Asilomar Conference on Signals*, Systems and Computers, 1994.

[23] J. A. Tropp and A. C. Gilbert, "Signal recovery from random measurements via Orthogonal Matching Pursuit," *IEEE Trans. Info. Theory*, Vol. 53, No. 12, 2007.

[24] M.R. Osborne, B. Presnell and B.A. Turlach, "A new approach to variable selection in least squares problems," *IMA Journal of Numerical Analysis*, Vol. 20, No. 3, 2000.

[25] R. Tibshirani, "Regression Shrinkage and Selection Via the Lasso," *Journal of the Royal Statistical Society*, Series B, Volume 58, 1994.